Amino Acids (2010) 38:929–936
DOI 10.1007/s00726-009-0301-4

ORIGINAL ARTICLE

NMR structural elucidation of myelin basic protein epitope 83–99 implicated in multiple sclerosis

Zinovia Spyranti · Theodore Tselios · George Deraos · John Matsoukas · Georgios A. Spyroulias

Received: 9 March 2009 / Accepted: 2 May 2009 / Published online: 26 May 2009
© Springer-Verlag 2009

Abstract Myelin basic protein peptide 83–99 (MBP83–99) is the most immunodominant epitope playing a significant role in the multiple sclerosis (MS), an autoimmune disease of the central nervous system. Many peptide analogues, linear or cyclic have been designed and synthesized based on this segment in order to inhibit the experimental autoimmune encephalomyelitis, the best well-known animal model of MS. In this study, the solution structural motif of $MBP_{83–99}$ has been performed using 2D ^{1}H-NMR spectroscopy in dimethyl sulfoxide. A rather extended conformation, along with the formation of a well defined α-helix spanning residues Val^{87}–Phe^{90} is proposed, as no long-range NOE are presented. Moreover, the residues of MBP peptide that are important for T-cell receptor recognition are solvent exposed. The spatial arrangement of the side chain all over the sequence of our NMR based model exhibits great similarity with the solid state model, while both TCR contacts occupy the same region in space.

Keywords MBP · Multiple sclerosis · NMR conformational analysis

Abbreviations

MS	Multiple sclerosis
CNS	Central nervous system
TCR	T-cell receptor
APL	Altered peptide ligand
EAE	Experimental autoimmune encephalomyelitis
MHC	Major histocompatibility complex
HLA	Human leukocyte antigens
MBP	Myelin basic protein
NMR	Nuclear magnetic resonance
NOE	Nuclear Overhauser effect
TOCSY	Total correlation spectroscopy
DYANA	Dynamic algorithm for NMR applications
RMSD	Root mean-square deviation
REM	Restrained energy minimization

Introduction

Multiple sclerosis (MS) is an inflammatory and demyelinating disease of the central nervous system (CNS) with environmental and genetic aetiology. Immune system faultily attacks and destroys the myelin sheath within the white matter of the brain and spinal cord, leading to inflammation (Steinman 1996). The recognition of antigenic peptides by T-cell receptors (TCRs) following the formation of the trimolecular complex major histocompatibility complex (MHC)–antigen (peptide)–TCR is the most important step in T-cell stimulation and MS induction (Mantzourani et al. 2005). High affinity of TCR for the MHC–antigen has been related with the agonistic activity of peptides derived

PDB codes: The 20 models ensemble along with the average energy minimized structure, have been deposited in Small Molecule Structure Deposition and their BMRB accession number is 20062.

Z. Spyranti · G. A. Spyroulias (✉)
Department of Pharmacy, University of Patras,
265 04 Panepistimioupoli, Rion, Greece
e-mail: g.a.spyroulias@upatras.gr

T. Tselios · G. Deraos · J. Matsoukas
Department of Chemistry, University of Patras,
265 04 Panepistimioupoli, Rion, Greece

from the immunodominant epitopes of myelin proteins (Davis et al. 1998).

In the body, the peptides adjust the most natural processes by binding with high selectivity to specific receptors and play an important role in the rational drug design (Mantzourani et al. 2008). New therapeutic approaches towards MS involve the use of altered peptide ligands (APLs) of disease-associated myelin epitopes to induce tolerance against T-Cell activation and myelin destruction. Antigen-specific therapies that target the encephalitogenic T cells leave the remainder of the immune system intact. APLs with critical TCR or MHC mutations could prevent the stimulation of T cells by deprivation of interaction between critical amino acids and of antigen and the TCR. Two phase II clinical trials using an APL derived from the $MBP_{83–99}$ epitope with substitutions mainly in the N terminus have been reported (Bielekova et al. 2000; Kappos et al. 2000). Both were stopped prematurely due to hypersensitivity reactions in one and disease exacerbation in the other. However, these trials demonstrated important points to novel therapeutic protocols with APLs based on the $MBP_{83–99}$ which is characterised as the most immunodominant epitope of myelin proteins.

NMR spectroscopy is well recognized as a powerful tool for the study of putative bioactive conformers of biologically important molecules (Pellecchia et al. 2008; Li et al. 2008; Zhou and Troy 2003, 2005). In this study, our goal was to examine the mean conformation of the immunodominant human epitope $MBP_{83–99,}$ identify common features that comprise a structural motif, and hence derive conclusions relevant to the physicochemical and structural properties required for biological activity. Experimental 2D NMR spectroscopic methods and structure calculations have been applied in order to obtain the mean structures in solution.

Results

Proton assignment

TOCSY maps were first analysed to assign the individual spin patterns of amino acids through scalar connectivities (Fig. 1).

Sequential, medium- and long-range connectivities were identified from NOESY maps acquired with $\tau_m = 300$ ms. Chemical shift for the $MBP_{83–99}$ peptide are reported in Table 1.

Numerous HN–HN sequential connectivities are detected in the region Glu^{83}–Asn^{84}, Val^{86}–Thr^{95} and Arg^{97}–Thr^{98}, while H_α–HN sequential connectivities are also identified between all residues, except prolines (Pro^{85}, Pro^{96} and Pro^{99}) (Fig. 1a, b, c). H_β–HN sequential connectivities are detected in peptide fragments including residues Glu^{83}–Asn^{84}, Val^{86}–Phe^{89}, Phe^{90}–Thr^{95} and Pro^{96}–Thr^{98}. An H_α-HN of (i, i + 2) type connectivity between Asn^{84}–Val^{86}, Pro^{85}–Val^{87}, Val^{87}–Phe^{89} and Asn^{92}–Val^{94}, as well as, a H_β–HN of (i, i + 2) type connectivity between residues Asn^{84}–Val^{86}, Val^{86}–His^{88} and Val^{87}–Phe^{89} has also been observed. A H_β–HN of (i, i + 2) type connectivity between residues His^{88}–Lys^{91} has also been identified. Numerous (i, i + 3) NOE connectivities have been observed between side chains protons all over the sequence.

Among the most characteristic NOEs are those between H_γ of Val^{86} with the side chain (H_γ) protons of Phe^{89}, H_ε of His^{88} with H_ζ protons of Lys^{91} as well as that between the HN and H_γ of Phe^{90} with the H_γ methyl protons of Val^{87}. Additionally, the NOE connectivities involving H_δ protons of Asn^{92} and H_α, H_β, H_γ and the amide proton of Thr^{95} confirm the close proximity of the two residues.

Structure calculations and conformational analysis

The average target function for the DYANA family of 20 calculated models (Fig. 2) was found to be 0.52 ± 0.08 Å^2 for $MBP_{83–99}$ models. No consistent violations existed at the final DYANA run and no constraint violation was found larger than 0.20 Å. The final REM models exhibit pairwise rmsd values for all residues 0.67 ± 0.27 Å (BB), 1.57 ± 0.41 Å (HA) for the 20 structures and 0.47 ± 0.18 Å (BB), 1.09 ± 0.27 Å (HA) for the mean structure, respectively (Table 2).

NMR solution structures

The NMR data for the $MBP_{83–99}$ peptide suggest a rather extended conformation for this analogue. Indeed, the absence of any long-range NOEs indicates the presence of a significant number of populations, where the $MBP_{83–99}$ analogue adopts a linear conformation. However, the observation of medium-range NOE connectivities at several parts of the peptide backbone identifies the existence of segments with local folded structure in the conformational ensemble. In particular, a backbone bend is formed by residues Asn^{92}–Thr^{95}, which is supported by some (i, i + 3) NOE connectivities between side chain protons of Asn^{92} and H_N, H_α, H_β, H_γ protons of Thr^{95}. Additionally, the phenyl ring of Phe^{90} is in close proximity with the backbone protons of Asn^{92}, (measured in energy minimized structure between 3.5 and 5 Å), as manifested by medium-range NOEs between the side chain protons (H_δ) of Phe^{90} with (1) H_N, H_α, H_β, and H_δ protons of Asn^{92} and (2) the side chain proton (H_γ) of Ile^{93}, indicating the formation of a second backbone bend (Figs. 2, 3).

Moreover, a helical conformation is identified involving residues Val^{87}–Phe^{90}. Despite the fact that not all the helix diagnostic NOEs are identified for this region, such as H_β

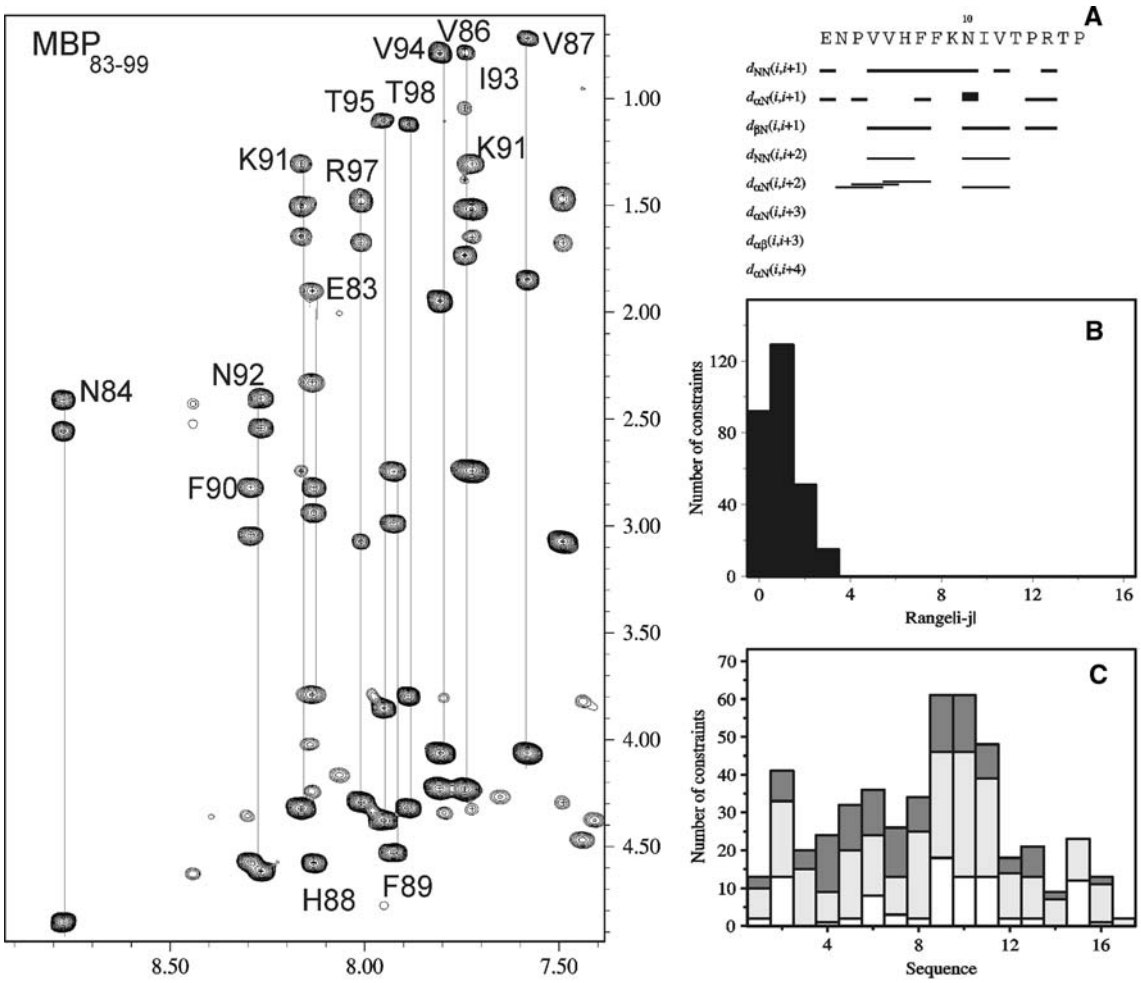

Fig. 1 Characteristic TOCSY fingerprints regions of linear $MBP_{83–99}$ extracted from 2D ^{1}H 600-MHz NMR recorded in DMSO-d_6 at 298 K (*left*). **a** Schematic representation of the sequential and medium-range NOE connectivities of $MBP_{83–99}$ peptide in DMSO. **b** Number of NOE constraints per residue for $MBP_{83–99}$. *White*, *gray* and *dark gray* *vertical bars* represent intraresidue, sequential and medium-range connectivities, respectively. **c** NOE range for $MBP_{83–99}$ peptide. All diagrams refer to meaningful NOE constraints extracted from τ_m = 300 ms NOESY (*right*)

His^{88}–H_N Lys^{91}, they are sufficient for the determination of a well defined α-helical structure, according to DYANA calculations.

As far as the nature of the peptide bond between Thr^{98} and Pro^{99} is concerned, ^{13}C resonances were observed for $MBP_{83–99}$ peptide, demonstrating the existence of a dominant conformation of the Thr^{98}–Pro^{99} peptide bond. C_β of Pro^{99} is found to be at 29.418 ppm, while C_γ is found at 24.836 ppm. The difference in ppm is 4.58, indicating that the dominant conformation of the bond of the model ensemble is *trans* and that *cis–trans* isomerization is not detectable in NMR time scale.

Concerning the isomeric status of the other prolines of the sequence, C_β of Pro^{85} is found to be at 29.066 ppm and C_β of Pro^{96} at 29.545 ppm, while C_γ is found at 24.744 ppm for Pro^{85} and at 24.860 for Pro^{96}, respectively. The difference in ppm is 4.32 for Pro^{85} and 4.685 for Pro^{96}, indicating that the dominant conformation is in both cases *trans*.

Discussion

The detailed conformational analysis, using spectroscopic studies, of linear agonist/antagonists analogues, $MBP_{87–99}$ (Mantzourani et al. 2008), [$Ala^{91,96}$] $MBP_{87–99}$ (Mantzourani et al. 2006) and [Arg^{91}, Ala^{96}] $MBP_{87–99}$ (Mantzourani et al. 2006), led to the identification of a common structural motif, which justified their antagonistic activity. The most important for TCR recognition amino acids, His^{88} and Phe^{89} present an altered topology in antagonist analogues [$Ala^{91,96}$] $MBP_{87–99}$ (Mantzourani et al. 2006) and [Arg^{91}, Ala^{96}] $MBP_{87–99}$ (Mantzourani et al. 2006), compared to agonist $MBP_{87–99}$ (Mantzourani et al. 2008);

Table 1 ^{1}H and ^{13}C chemical shifts (ppm) of the residues in the $MBP_{83–99}$ peptide at 298 K (DMSO-d_6)

Residue		HN	Hα/**Cα**	Hβ/**Cβ**	Other
83	Glu	8.135	3.788	2.326	γCH_3 1.901
			51.690	**29.349**	**26.936**
84	Asn	8.772	4.850	2.556, 2.409	δNH_2 7.398, 6.958
			48.385	**37.011**	
85	Pro	–	4.190	2.133, 1.924	Hγ 1.844; Hδ 3.784, 3.631
			58.873	**29.066**	**24.744**; **47.615**
86	Val	7.808	4.058	1.948	γCH_3 0.789
			58.237	**30.524**	**19.635**; **18.682**
87	Val	7.584	4.059	1.847	γCH_3 0.723
			58.225	**30.683**	**19.375**; **18.480**
88	His	8.131	4.572	2.935, 2.820	Hδ2 7.188; Hε1 8.910
			51.503	**27.655**	**117.151**; **134.146**
89	Phe	7.927	4.527	2.984, 2.745	Hδ 7.153; Hε 7.231; Hζ 7.172
			53.984	**37.961**	**129.562**; **128.380**; **126.776**
90	Phe	8.291	4.567	3.040, 2.817	Hδ 7.170; Hε 7.231; Hζ 7.229
			54.103	**37.900**	**129.618**; **128.494**; **126.804**
91	Lys	8.162	4.321	1.646, 1.528	Hγ 1.307; δCH_3 1.496; εCH_3 2.743; Hζ 7.726
			52.436	**32.216**	**22.524**; **27.152**; **39.141**
92	Asn	8.266	4.613	2.544, 2.404	δNH_2 7.507, 7.014
			50.053	**37.086**	
93	Ile	7.745	4.227	1.736	Hγ 1.380, 1.048; γCH_3 0.806; δCH_3 0.771
			57.431	**37.233**	**24.404**; **15.707**; **11.525**
94	Val	7.809	4.224	1.947	ΓCH_3 0.794
			57.600	**30.691**	**19.587**; **18.653**
95	Thr	7.952	4.376	3.850	γCH_3 1.108
			57.123	**67.022**	**19.749**
96	Pro	–	4.331	2.028, 1.893	Hγ 1.806; Hδ 3.778, 3.611
			59.778	**29.545**	**24.860**
97	Arg	8.011	4.291	1.677, 1.494	Hγ 1.456; Hδ 3.071; Hε 7.493
			52.163	**29.344**	**25.237**; **40.754**
98	Thr	7.890	4.317	3.794	γCH_3 1.123
			57.292	**67.384**	**19.749**
99	Pro	–	4.412	1.997, 1.872	Hγ 1.819; Hδ 3.659, 3.619
			59.828	**29.418**	**24.836**; **47.314**

they remain buried in the MHC groove (Mantzourani et al. 2007) and are not available for recognition and interaction with the TCR. It was the first attempt to gain a better understanding of the molecular recognition mechanisms that underlie TCR antagonism by these APLs.

The NMR data of $MBP_{83–99}$ presented in this study indicate an extended conformation for this analogue, which found to be in agreement with X-ray crystallography data (Hahn et al. 2005). Recent crystallographic structure of a trimolecular complex of $MBP_{83–99}$, HLA-DRB1*1501 and a human TCR isolated from a patient with relapsing–remitting MS revealed an extended conformation with His^{88}, Phe^{89} and Lys^{91} residues identified as major TCR contact residues for human MBP-specific T-cell clones, observed to be solvent exposed and accessible for recognition by TCR. The lack of any long-range NOE in our model is consistent with the extended conformation of the analogue. However, identification of a number of medium-range NOE at different parts of the peptide backbone suggests the presence of populations with segments of local folded structure in the conformational ensemble, such as the formation of a backbone bend in the His^{88}–Phe^{90} and Asn^{92}–Thr^{95} segments. These bends in the middle of the sequence lead to a more compact backbone conformation in solution. Another difference between the two conformations exists; regarding the formation of an α-helix spanning residues Val^{87}–Phe^{90}, observed only in the case of the NMR derived structure. Despite of these differences,

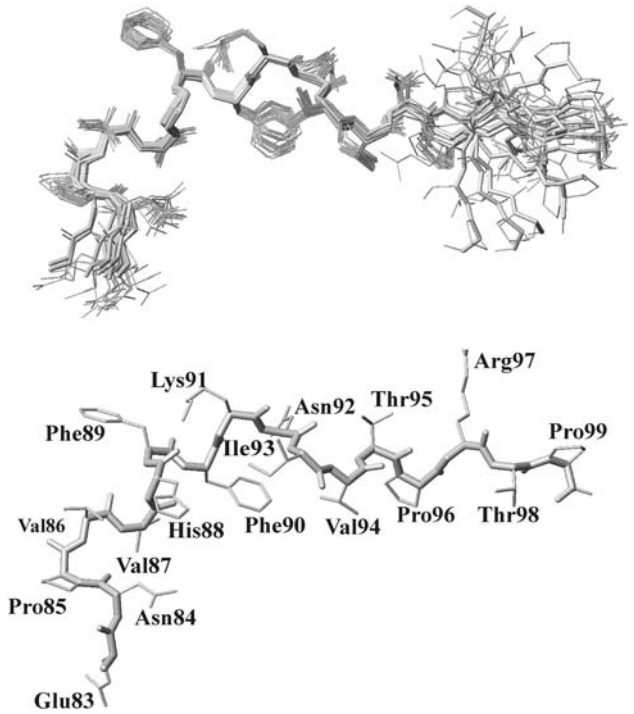

Fig. 2 The family of 20, energy minimized, DYANA models calculated for the $MBP_{83–99}$ analogue (*top*) and the mean energy minimized $MBP_{83–99}$ structure (*bottom*). Figures were generated with the MOLMOL program

Table 2 Statistical analysis for the final REM structures of the $MBP_{83–99}$ peptide

	$MBP_{83–99}$	
	REM (20 structures)	<REM>
RMS violations per experimental distance constraints (Å)[a]		
Intraresidue (92)	0.0248 ± 0.0030	0.0246
Sequential (129)	0.0217 ± 0.0024	0.0172
Medium-range (66)	0.0241 ± 0.0040	0.0203
Total (287)	0.0234 ± 0.0015	0.0205
Average number of violations per structure		
Intraresidue	7.50 ± 1.3964	7.0
Sequential	7.35 ± 1.7400	5.0
Medium-range	3.50 ± 1.3601	3.0
Total	18.35± 1.7400	15.0
Structural analysis		
Average no. of NOE violations greater than 0.3 Å	0.000 ± 0.00	0.00
Largest residual NOE violation (Å)	0.206	0.140
Average distance penalty function ($Å^2$)	0.178 ± 0.002	0.146
Amber energy (kJ mol^{-1})	−323.85 ± 10.79	−324.69

[a] Numbers in parenthesis indicate the number of meaningful upper distance limits per class

the overall fold of the $MBP_{83–99}$ peptide exhibits remarkable similarities in the solid state and in solution.

The spatial arrangement of the side chain all over the sequence of our NMR-based model exhibits great similarity with the solid state model. Both TCR contacts occupy the same region in space. In particular, the imidazole and phenyl ring of His^{88} and Phe^{89}, respectively, remain solvent exposed in both models (Fig. 4). Phe^{90}, the primary MHC contact, remains in exactly the same position and the phenyl ring presents the same orientation as in the X-ray model.

In a previous publication of our group (Spyranti et al. 2007), a model of the cyclo (87–99) $MBP_{87–99}$ peptide was proposed. Despite the cyclic nature of this peptide and the significant structural differences among the cyclo (87–99) $MBP_{87–99}$ and the linear $MBP_{83–99}$, presented in this study, common structural characteristics are to be found, regarding the spatial arrangement of the side chains. Chemical shift difference plots regarding Cα and Cβ atoms of the backbone illustrate quite significant variations due to different structural conformations, but the chemical variations are almost eliminated as far as the side chains are concerned (data not shown). The primary TCR contacts, His^{88} and Phe^{89} occupy the same region in space. Furthermore, the relative orientation of the imidazole ring of His^{88} and phenyl ring of Phe^{89} is conserved in both analogues. Regarding the phenyl ring of the primary MHC contact, Phe^{90}, it lies within the same region in space, but presents an altered orientation (Fig. 5).

Moreover, 3D NMR structures of $MBP_{81–98}$ have been obtained by Fares et al. (2006) in (a) an aqueous solution, (b) a mixture of trifluroethanol and water (TFE-d_2) and (c) a dispersion of 100 mM dodecylphosphocholine (DPC-d_{38}). In the $MBP_{81–98}$ fragment, this epitope forms a stable, amphipatic, α-helix under organic and membrane-mimetic conditions, but has only a partially helical conformation in aqueous solution. The $MBP_{83–99}$ model presented in our study partially resembles the structure of $MBP_{81–98}$ in aqueous solution. However, the proposed model of Fares et al. forms a relatively stable core and suggests a weakly helical conformation in the region Val^{86}–Phe^{90}, while the presented NMR data suggest the formation of a well-structured α-helix for residues Val^{87}–Phe^{90}. The obtained differences among the structures can be rationalized from the nature of the solvent. In general, the organic solvent TFE is electrically neutral and preferentially aggregates around the polypeptide, displacing water, and thereby forming a low dielectric environment that favours the formation of intrapeptide hydrogen bonds (Roccatano et al. 2002). On the other hand, the zwitterionic DPC provides not only a hydrophobic surface from its acyl chain, but both positive- and negative-charge contacts to the polypeptide

Fig. 3 The family of 20, energy minimized, DYANA models calculated for the $MBP_{83–99}$ analogue, illustrated as ribbon. Figure was generated with the MOLMOL program

chain, allowing it to adopt a much more relaxed conformation The significant role of the charges in stabilizing the conformation has been demonstrated in more detail in our work towards more stable MBP cyclic analogues in the treatment of multiple sclerosis (MS) (Deraos et al. 2008; Katsara et al. 2009). As a conclusion, the solvent can elicit structural changes and thus only a minimal direct comparison can be made with the above mentioned conformational ensembles of the MBP segment.

Materials and methods

Peptide synthesis and purification

Linear epitope $MBP_{83–99}$, was synthesized step by step by Fmoc/tBu methodology using 2-chlorotrityl chloride (CLTR-Cl) resin (0.7 mmol Cl^{-}/g) and N^{α}-Fmoc (9-fluorenylmethyloxycarboxyl)-protected amino acids [Fmoc-Thr(tBu)-OH, Fmoc-Arg(Pbf)-OH, Fmoc-Pro-OH, Fmoc-Val-OH, Fmoc-Ile-OH, Fmoc-Asn-OH,, Fmoc-Lys (Boc)-OH, Fmoc-Phe-OH, Fmoc-His(Trt)-OH, Fmoc-Val-OH, Fmoc-Glu(tBu)-OH] as previously described (Tselios et al. 1999, 2000, 2002; Matsoukas et al. 2005). In general, the Fmoc-Pro-OH was esterified on the resin in the presence of diisopropylethylamine (DIPEA) in DCM. In each case, the

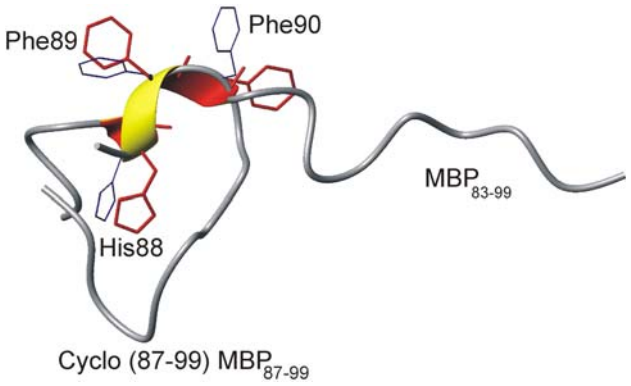

Fig. 5 Superimposition of the cyclo (87–99) $MBP_{87–99}$ and the linear $MBP_{83–99}$ peptide illustrated as ribbon

Fmoc deprotection and coupling were achieved using piperidine solution and N,N′-diisopropylcarbodiimide (DIC)/1-hydroxybenzotriazole (HOBt) as coupling regents, respectively. The Kaiser test and thin layer chromatography (TLC) in *n*-butanol/acetic acid/water (4:1:1) (BAW) as elutant verified the completeness of each Fmoc deprotection or coupling. The protected peptide–resin was treated with the splitting mixture DCM/TFE (7/3) to remove peptide from the resin and the final deprotection was carried out usin TFA solution in the presence of 1,2-ethanedithiol/anisole as scavengers. The purification and identification of peptide were achieved using reverse phase high performance liquid chromatography (RP-HPLC, semi preparative elution) and electron spray ionization (ESI) mass spectrometry, respectively (Tselios et al. 1999, 2000, 2002; Matsoukas et al. 2005). Dimethylsulfoxide DMSO-d_6 (MERCK) was used as deuterated solvent in NMR experiments (Vesterman et al. 1989) and the peptide was dissolved to a final concentration of 2–2.5 mM in order to record 1D and 2D NMR spectra. The NMR studies have been performed in DMSO in conjunction with previous studies of other MBP peptide analogues, mimicking a prototypical hydrophobic environment.

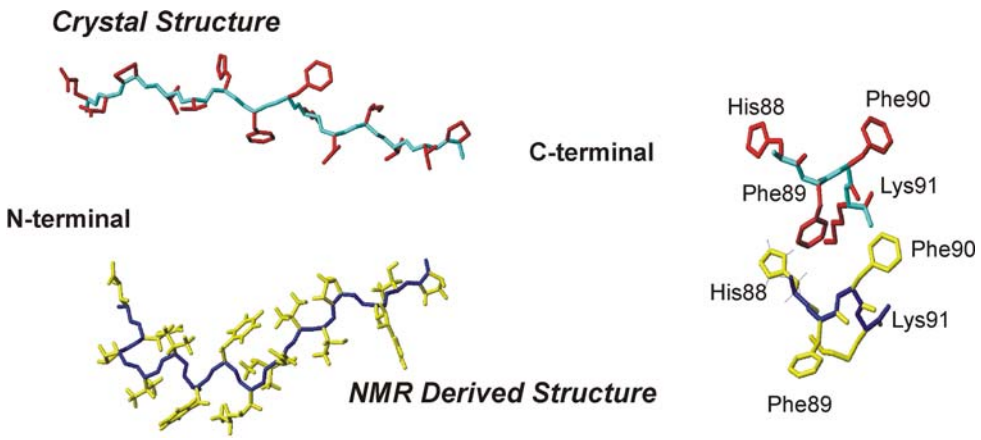

Fig. 4 Backbone representation of crystal structure (*top*) and NMR derived structure (*bottom*) of the $MBP_{83–99}$ peptide and orientation of the side chains of MHC anchors, Asn^{92}, Ile^{93}, and Thr^{95}, as well as TCR contacts, His^{88} and Phe^{89}. (*left*). Schematic representation of the side chain of His^{88}-Phe^{89}-Phe^{90}-Lys^{91} for the X-ray structure (*top*) and the energy minimized NMR (*bottom*) structure of $MBP_{83–99}$ peptide (*right*). Figures were generated with the MOLMOL program

NMR spectroscopy

Data were acquired at 298 K on a Bruker Avance 600 and 700-MHz spectrometer. ^{1}H 1D NMR spectra were recorded using spectral width of 12–17 ppm with or without presaturation of the H_2O signal. ^{1}H–^{1}H 2D TOCSY (Braunschweiler and Ernst 1983; Bax and Davis 1985) (Fig. 1), was recorded using the MLEV-17 spin lock sequence using $\tau_m = 80$ ms, and ^{1}H–^{13}C HSQC (Bax and Grzesiek 1993; Bothner-By et al. 1984) with 200.791-ppm spectral width in F1. ^{1}H–^{1}H TPPI NOESY (Marion and Wüthrich 1983; Jeener et al. 1979) spectra was acquired using mixing time $\tau_m = 300$ ms applying water suppression during the relaxation delay and mixing time. All 2D spectra were acquired with 10.014-ppm spectral width, consisting of 2-K data points in the F2 dimension, 16–32 transients and 512–1,024 complex increments in the F1 dimension. Raw data were multiplied in both dimensions by a pure cosine-squared bell window function and Fourier-transformed to obtain 2,048 × 2,048 real data points. A polynomial base-line correction was applied in both directions. For data processing and spectral analysis, the standard Bruker software (XWinNMR 3.5) and XEASY program (Eccles et al. 1991) (ETH, Zurich) were used.

NOE constraints

A total of 776 NOESY cross-peaks were assigned in both dimensions for the $MBP_{83–99}$ peptide in DMSO. The number of unique cross-peaks was 401, that is 24 constraints per residue. Their intensities were converted into upper limit distances through CALIBA (Güntert et al. 1991). Sequential constraints, number and range of NOEs are illustrated in Fig. 1.

Structure calculations and refinement

The NOE-derived structural information extracted from the analysis of NOESY spectrum acquired in DMSO-d_6 solutions under identical experimental conditions for the $MBP_{83–99}$ peptide and was introduced to DYANA (Güntert et al. 1997; Wüthrich et al. 1983) software for structure calculation. The family ensemble of 20 best DYANA models for the linear peptide (out of 400 calculated) in terms of target function (<0.4 Å^2) and NOE violations (<0.2 Å) were submitted to energy minimization through REM [AMBER 5.0 (Pearlman et al. 1997), SANDER (Pearlman et al. 1991) program]. A force constant of 133.76 kJ mol^{-1} Å^2 is applied for the distance constraints. MBP peptide models are illustrated in Fig. 3 (figures are generated with MOLMOL (Koradi et al. 1996). Structural calculations have been performed on IBM RISC6000 and xw4100/xw4200 HP Linux workstations. The 20 models ensemble and the mean structure of $MBP_{83–99}$, analogue are illustrated in Fig. 2.

Acknowledgments This work was financially supported by the Greek General Secretariat of Research and Technology, Greece. G.A.S. and Z.S. wish to acknowledge a short-term EMBO grant (ASTF 99-2004) and EU-NMR program, Contract # RII3-026145 (CERM; Center of Magnetic Resonance, University of Florence) for access to NMR instrumentation.

References

Bax A, Davis DG (1985) MLEV-17-based two-dimensional homonuclear magnetization transfer spectroscopy. J Magn Reson 65:355–360

Bax A, Grzesiek S (1993) Methodological advances in protein NMR. Acc Chem Res 26:131–138

Bielekova B, Goodwin B, Richert N, Cortese I, Kondo T, Afshar G, Gran B, Eaton J, Antel J, Frank JA, McFarland HF, Martin R (2000) Encephalitogenic potential of the myelin basic protein peptide (amino acids 83–99) in multiple sclerosis: results of a phase II clinical trial with an altered peptide ligand. Nat Med 6:1167–1175

Bothner-By AA, Stephens RL, Lee JM, Warren CD, Jeanloz RW (1984) Structure determination of a tetrassacharide: transient nuclear Overhauser effect in the rotating frame. J Am Chem Soc 106:811–813

Braunschweiler L, Ernst RR (1983) Coherence transfer by isotropic mixing: application to proton correlation spectroscopy. J Magn Reson 53:521–528

Davis MM, Boniface JJ, Reich Z, Lyons D, Hampl J, Arden B, Chien YH (1998) Ligand recognition by alpha beta T cell receptors. Annu Rev Immunol 16:523–544

Deraos G, Chatzantoni K, Matsoukas MT, Tselios T, Deraos S, Katsara M, Papathanasopoulos P, Vynios D, Apostolopoulos V, Mouzaki A, Matsoukas J (2008) Citrullination of linear and cyclic altered peptide ligands from myelin basic protein (MBP87–99) epitope elicits a Th1 polarized response by T cells isolated from multiple sclerosis patients: implications in triggering disease. J Med Chem 51(24):7834–7842

Eccles C, Güntert P, Billeter M, Wüthrich K (1991) Efficient analysis of protein 2D NMR spectra using the software package EASY. J Biomol NMR 1:111–130

Fares C, Libich DS, Harauz G (2006) Solution NMR structure of an immunodominant epitope of myelin basic protein. FEBS J 273:601–614

Güntert P, Braun W, Wüthrich K (1991) Efficient computation of three-dimensional protein structures in solution from nuclear magnetic resonance data using the program DIANA and the supporting programs CALIBA, HABAS and GLOMSA. J Mol Biol 217:517–530

Güntert P, Mumenthaler C, Wüthrich K (1997) Torsion angle dynamics for NMR structure calculation with the new program DYANA. J Mol Biol 273:283–298

Hahn M, Nicholson MJ, Pyrdol J, Wucherpfennig KW (2005) Unconventional topology of self peptide–major histocompatibility complex binding by a human autoimmune T cell receptor. Nat Immunol 6:490–496

Jeener J, Meier BH, Bachmann P, Ernst RR (1979) Investigation of exchange processes by two-dimensional NMR spectroscopy. J Chem Phys 71:4546–4553

Kappos L, Comi G, Panitch H, Oger J, Antel J, Conlon P, Steinman L (2000) The Altered Peptide Ligand in Relapsing MS Study

Group. Induction of a non-encephalitogenic type 2 T helper-cell autoimmune response in multiple sclerosis after administration of an altered peptide ligand in a placebo-controlled, randomized phase II trial. Nat Med 6:1176–1182

Katsara M, Deraos G, Tselios T, Matsoukas MT, Friligou I, Matsoukas J, Apostolopoulos V (2009) Design and synthesis of a cyclic double mutant peptide (cyclo(87–99)[A91, A96]MBP87–99) induces altered responses in mice after conjugation to mannan: implications in the immunotherapy of multiple sclerosis. J Med Chem 52(1):214–218

Koradi R, Billeter M, Wüthrich K (1996) MOLMOL: a program for display and analysis of macromolecular structures. J Mol Graph 14:51–55

Li X, Peterkofsky A, Wang G (2008) Solution structure of NPr, a bacterial signal-transducing protein that controls the phosphorylation state of the potassium transporter-regulating protein IIANtr. Amino Acids 1438–2199(35):531–539

Mantzourani ED, Mavromoustakos TM, Platts JA, Matsoukas JM, Tselios T (2005) Structural requirements for binding of myelin basic protein (MBP) peptides to MHC II: effects on immune regulation. Curr Med Chem 12:1521–1535

Mantzourani ED, Tselios TV, Grdadolnik SG, Platts JA, Brancale A, Deraos G, Matsoukas JM, Mavromoustakos TM (2006a) Comparison of proposed putative active conformations of linear altered peptide ligands of myelin basic protein epitope 87–99 by spectroscopic and modelling studies: the role of position 91 and 96 in T-cell receptor activation. J Med Chem 49:6683–6691

Mantzourani ED, Tselios TV, Grdadolnik SG, Brancale A, Platts JA, Matsoukas JM, Mavromoustakos TM (2006b) A putative bioactive conformation for the altered peptide ligand of myelin basic protein and inhibitor of experimental autoimmune encephalomyelitis [Arg91, Ala96] MBP87–99. J Mol Graph Mod 25:17–29

Mantzourani ED, Platts JA, Brancale A, Mavromoustakos TM, Tselios TV (2007) Molecular dynamics at the receptor level of immunodominant myelin basic protein epitope 87–99 implicated in multiple sclerosis and its antagonists altered peptide ligands: triggering of immune response. J Mol Graphics Modell 26:471–481

Mantzourani ED, Laimou D, Matsoukas MT, Tselios T (2008a) Peptides as therapeutic agents or drug leads for autoimmune, hormone dependent and cardiovascular diseases. Anti-inflamm Anti-allergy Agents Med Chem 4:294–306

Mantzourani ED, Blokar K, Tselios TV, Matsoukas JM, Platts JA, Mavromoustakos TM, Grdadolnik SG (2008b) A combined NMR and molecular dynamics simulation study to determine the conformational properties of agonists and antagonists against experimental autoimmune encephalomyelitis. Bioorg Med Chem 16:2171–2182

Marion D, Wüthrich K (1983) Application of phase sensitive two-dimensional correlated spectroscopy (COSY) for measurements of 1H–1H spin–spin coupling constants in proteins. Biochem Biophys Res Commun 113:967–974

Matsoukas J, Apostolopoulos V, Kalbacher H, Papini AM, Tselios T, Chatzantoni K, Biagioli T, Lolli F, Deraos S, Papathanassopoulos P, Troganis A, Mantzourani E, Mavromoustakos T, Mouzaki A (2005) Design and synthesis of a novel potent myelin basic protein epitope 87–99 cyclic analogue: enhanced stability and biological properties of mimics render them a potentially new class of immunomodulators. J Med Chem 48:1470–1480

Pearlman DA, Case DA, Caldwell GC, Siebel GL, Singh UC, Weiner P, Kollman PA (1991) AMBER 4.0. University of California, San Francisco

Pearlman DA, Case DA, Caldwell JW, Ross WS, Cheatham TE, Ferguson DM, Seibel GL, Singh UC, Weiner PK, Kollman PA (1997) AMBER 5.0. University of California, San Francisco

Pellecchia M, Bertini I, Cowburn D, Dalvit C, Giralt E, Jahnke W, James TL, Homans SW, Kessler H, Luchinat C, Meyer B, Oschkinat H, Peng J, Schwalbe H, Siegal G (2008) Perspectives on NMR in drug discovery: a technique comes of age. Nat Rev Drug Discov 7(9):738–745

Roccatano D, Colombo G, Fioroni M, Mark (2002) Mechanism by which 2,2,2-trifluorethanol/water mixtures stabilize secondary structure formation in peptides: a molecular dynamics study. Proc Natl Acad Sci 99:12179–12184

Spyranti Z, Dalkas GA, Spyroulias GA, Mantzourani ED, Mavromoustakos T, Friligou I, Matsoukas JM, Tselios TV (2007) Putative bioactive conformations of amide linked cyclic myelin basic protein peptide analogues associated with experimental autoimmune encephalomyelitis. J Med Chem 50(24):6039–6047

Steinman L (1996) Multiple sclerosis: a coordinated immunological attack against myelin in the central nervous system. Cell 85:299–302

Tselios T, Probert L, Daliani I, Matsoukas E, Troganis A, Gerothanassis I, Mavromoustakos T, Moore G, Matsoukas J (1999) Design and synthesis of a potent cyclic analogue of the myelin basic protein epitope MBP72–85: importance of the Ala81 carboxyl group and of a cyclic conformation for induction of experimental allergic encephalomyelitis. J Med Chem 42:1170–1177

Tselios T, Daliani I, Deraos S, Thymianou S, Matsoukas E, Troganis A, Gerothanassis I, Mouzaki A, Mavromoustakos T, Probert L, Matsoukas J (2000) Treatment of experimental allergic encephalomyelitis (EAE) by a rationally designed cyclic analogue of myelin basic protein (MBP) epitope 72–85. J Bioorg Med Chem Lett 10:2713–2717

Tselios T, Apostolopoulos V, Daliani I, Deraos S, Grdadolnik S, Mavromoustakos T, Melachrinou M, Thymianou S, Probert L, Mouzaki A, Matsoukas J (2002) Antagonistic effects of human cyclic MBP(87–99) altered peptide ligands in experimental allergic encephalomyelitis and human T-cell proliferation. J Med Chem 45:275–283

Vesterman B, Saulitis J, Betins J, Liepins E, Nikiforovich GV (1989) Dynamic space structure of the Leu-enkephalin molecule in DMSO solution. Biochim Biophys Acta 998:204

Wüthrich K, Billeter M, Brown W (1983) Pseudo-structures for the 20 common amino acids for use in studies of protein conformations by measurements of intramolecular proton-proton distance constraints with nuclear magnetic resonance. J Mol Biol 169:949–961

Zhou GP, Troy FA (2003) Characterization by NMR and molecular modeling of the binding of polyisoprenols (PI) and polyisoprenyl recognition sequence (PIRS) peptides: three-dimensional structure of the complexes reveals sites of specific interactions. Glycobiology 13:51–57

Zhou GP, Troy FA (2005) NMR studies on how the binding complex of polyisoprenol recognition sequence peptides and polyisoprenols can modulate membrane structure. Curr Protein Pept 6:399–411